

A comparison of surface sensitive reflection spectroscopies

This article has been downloaded from IOPscience. Please scroll down to see the full text article.

2004 J. Phys.: Condens. Matter 16 S4279

(<http://iopscience.iop.org/0953-8984/16/39/003>)

View [the table of contents for this issue](#), or go to the [journal homepage](#) for more

Download details:

IP Address: 129.252.86.83

The article was downloaded on 27/05/2010 at 17:55

Please note that [terms and conditions apply](#).

A comparison of surface sensitive reflection spectroscopies

D S Roseburgh¹ and R J Cole

School of Physics and Centre for Materials Science and Engineering, James Clerk Maxwell Building, Mayfield Road, King's Buildings, University of Edinburgh, Edinburgh EH9 3JZ, UK

E-mail: d.roseburgh@ed.ac.uk

Received 27 April 2004

Published 17 September 2004

Online at stacks.iop.org/JPhysCM/16/S4279

doi:10.1088/0953-8984/16/39/003

Abstract

The surface sensitivity (in the sub-nanometre regime) of reflection spectroscopies is discussed. Simulations are used to illustrate the strengths and limitations of 45 degree reflectometry (45DR). Particular emphasis is placed upon the comparison with spectroscopic ellipsometry.

(Some figures in this article are in colour only in the electronic version)

1. Introduction

Light reflected from the surface of a material contains information about the nature of that surface. But even for metals consideration of typical absorption coefficients suggests that incident light interacts with the top $\gtrsim 10^2$ atomic layers. Thus optical reflectivity is not considered by the surface science community, where surface properties are studied at the atomic scale, to be 'surface sensitive'. This fact is readily illustrated by the reflectivity simulations shown in figure 1. It is apparent that overlayers several nanometres thick modify the reflectivity only weakly, and we must conclude that reflectivity measurements are poorly suited to studying surface reconstructions or monolayer adsorbates.

A secondary problem is that the reflection spectra of solids tend to be rather broad and featureless. However, their derivatives with respect to external parameters such as electric field, mechanical stress and temperature clearly reveal critical point energies. This fact is exploited by 'modulation' techniques [1] which focus on the change in reflectivity induced in this way. Modulation spectroscopy is conveniently and advantageously implemented by modulating the external parameter at some known frequency, ω , and using a lock-in amplifier to detect the resulting oscillations in optical response (known as 'phase-sensitive detection'). Since the temporal dependence of the intensity of the detected light has the form $\sum_{n=0}^{\infty} I_{n\omega}$, measuring the ratios $I_{n\omega}/I_{n'\omega}$ provides a normalized measure of the change in reflectivity, i.e. $\delta R/R$.

¹ Author to whom any correspondence should be addressed.

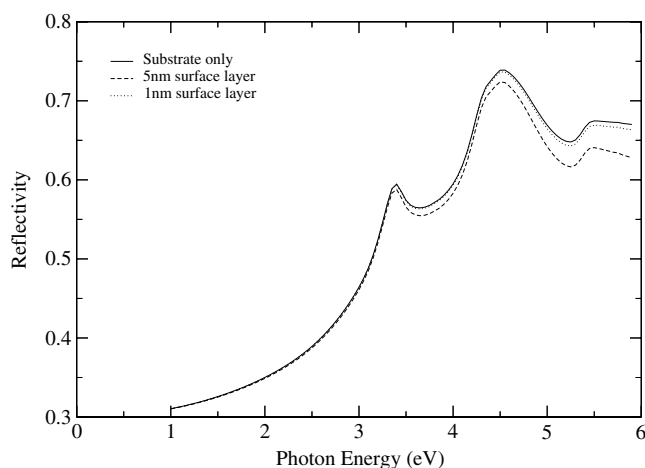


Figure 1. Calculated normal incidence reflectivity of SiO₂ thin films on a Si substrate.

Instrumental uncertainties can be eliminated by such ‘ratiometric’ measurements and hence $\delta R/R$ can be measured much more accurately than R itself. This improvement in signal to noise enables monolayer effects to be detected. This principle can be seen, for example, in the work of Gaigalas and co-workers [2] using electroreflectance to study submonolayer coverages of molecular adsorbates.

Spectroscopic ellipsometry (SE) is another ratiometric modulation technique [3]. In this case the sample is not modified, but rather the polarization of the incident light is modulated between the s and p states, and r_p/r_s is measured. (r are complex Fresnel reflection amplitudes and are related to the corresponding reflectivities, R , by $R = |r|^2$.) Although the ellipsometric ratio of ultra-thin (i.e. sub-nanometre) films is determined predominantly by the substrate, the ratiometric nature of ellipsometry allows submonolayer sensitivity to be achieved [4].

More recently (see [5] for a review), a variety of ways have been devised for directly measuring surface effects in optical reflectivity. In surface differential reflectivity (SDR), pioneered by Chiaradia and co-workers [6–8], the incident light is split (in time, using a chopper) between two identical samples, one of which is then modified, for example by adsorption. The intensity of the reflected light has the form $I_0 + I_\omega$, where ω is the frequency of the chopper, and the ratio I_ω/I_0 is directly proportional to $\Delta R/R$, the fractional difference in reflectivity of the two samples. Thus SDR is ratiometric and also *surface specific*. SDR provided the first conclusive demonstration of the use of reflectivity spectra in the detection of surface states. The technique, however, is not applicable if a reference surface is not available.

An alternative approach to surface specificity is the exploitation of symmetry, as exemplified by second-harmonic generation (SHG) [5]. While centro-symmetric materials have a null second order polarizability, this symmetry is necessarily broken at a surface. Thus second order reflection (i.e. light reflected with double the frequency of the incident light) is derived specifically from the surface. Second harmonic signals are weak and so laser (or synchrotron) excitation is required. While tunable lasers (such as the Ti-sapphire) are becoming quite widespread, here we concentrate on linear optical techniques which utilize conventional broadband light sources.

Reflection anisotropy spectroscopy (RAS) measures the quantity

$$\frac{\Delta r}{r} = 2 \frac{r_x - r_y}{r_x + r_y}, \quad (1)$$

the anisotropy in the normal incidence Fresnel reflection amplitudes for two orthogonal linear polarizations. RAS is another ratiometric polarization modulation technique (it can be regarded as the normal incidence limit of ellipsometry) and has a detection limit of $\sim 10^{-5}$, enabling small anisotropies to be detected. For isotropic solids any observed reflection anisotropy must be derived from the surface, hence surface specificity is achieved in this case.

Of course the symmetry properties which endow techniques such as SHG and RAS with surface specificity also bring limitations. For example, all laterally isotropic surfaces are ‘RAS inactive’. Recently, Bleckman *et al* have proposed a new reflection spectroscopy which is surface specific without imposing symmetry constraints on the surface [9]. This technique, known as 45 degree reflectometry (45DR), relies on a particular feature of the Fresnel equations: for reflection from a mathematically abrupt semi-infinite substrate at 45 degree incidence, $R_s^2 = R_p$. Thus the departure of surface optical properties from the bulk optical response is signalled by non-zero Δ_{45} , defined by

$$\Delta_{45} = R_s^2 - R_p. \quad (2)$$

Its surface specificity and versatility lead Aspnes, a pioneer of surface optical spectroscopy, to refer to 45DR as ‘an exciting prospect’ [10], yet the technique has received only limited attention [11–15]. One reason is immediately apparent: quantities such as Δ_{45} do not lend themselves to ratiometric measurement. Instead one must construct Δ_{45} from separate measurements of R_s and R_p , which must therefore be measured with high absolute accuracy. In this work the strengths and weaknesses of 45DR in comparison with other reflection spectroscopies are investigated. We by-pass the experimental difficulties of accurately measuring Δ_{45} by using simulations.

2. Simulation details

In this work we consider the reflection of light from stratified systems, i.e. systems consisting of homogeneous layers separated by abrupt interfaces parallel to the surface. The reflection of arbitrarily polarized light from a multilayer consisting of arbitrarily aligned anisotropic media can be described using the 4×4 matrix method first reported by Teitler and Henvis [16], popularized by Berreman [17, 18] and reviewed in [3] and [19]. In this approach a 4×4 ‘partial transfer matrix’, T_p , relates E_x , E_y , H_x , H_y , the amplitudes of the electric and magnetic fields parallel to the interfaces, at the upper and lower surfaces of each layer. T_p^i is determined by the angle of incidence from the ambient and the dielectric matrix of layer i . Since the in-plane field amplitudes are conserved at the interfaces, multiplication of a series of partial transfer matrices gives a matrix connecting the field amplitudes incident upon and exiting the multilayer. Converting to the sp basis to describe the field amplitudes in the incident medium and substrate gives a total transfer matrix, T , with the form

$$T = L_a^{-1} \left[\prod_i T_p^i \right] L_b. \quad (3)$$

The Jones reflection matrix [20, 3] can easily be obtained from T , enabling reflectivity, ellipsometry, 45DR and RAS spectra to be simulated. This is a flexible method, allowing an arbitrary number of surface layers and any angle of incidence. Its numerical implementation has been discussed very clearly by Schubert [19].

We confine our attention to essentially two archetypal substrate materials: the semiconductor Si and the metal Au. While the reflectivity spectra of ‘bare’ substrates can be simulated, perfect interfaces between vacuum and bulklike materials do not exist. Atomic relaxation, if not surface reconstruction, is present at all real surfaces, leading to distinct optical

properties. Indeed it is the aim of surface optical spectroscopy to probe precisely this modified surface region. Such real surfaces can be modelled in the stratified media formalism by the introduction of a layer with distinct optical properties between substrate and ambient. For simplicity ultra-thin films of SiO₂ (in the case of Si) and Cu (in the case of Au) play the role of ‘the surface’ in simulations reported in this work.

3. Results and discussion

3.1. Reflectivity

The simulated normal incidence reflectivity of oxidized Si is shown in figure 1. The calculations assumed a semi-infinite Si substrate beneath a thin film of SiO₂, and the optical constants of Si and SiO₂ were taken from [22]. As mentioned in section 1, overlayers with thickness of ~ 1 nm (i.e. several monolayers) have a small effect on R , particularly in this case in the non-absorbing energy regime. A route to enhanced surface sensitivity can be seen in figure 2 which shows as solid curves R_s and R_p for Si and Au as functions of the angle of incidence ϕ . The dashed curves are the corresponding results when overlayers of SiO₂ and Cu are added to the Si and Au substrates, respectively. To ensure the surface effects are visible, overlayer thicknesses of 5 nm were used. In all cases a photon energy of 3 eV is assumed. Again the surface effects are rather modest but for p polarization the reflectivity goes through a minimum at the pseudo-Brewster angle ϕ_B and the ‘substrate reflectivity’ is suppressed, particularly for non-absorbing media. Surface photoabsorption (SPA), developed by Kobayashi and Horikoshi [21], exploits this effect by implementing a form of SDR that employs p polarized light at near Brewster incidence. In SPA a single sample is modified in a periodic manner, for example by epitaxial growth, and the fractional change in reflectivity is detected. For absorbing media, tuning the incidence angle does not produce significant enhancement of surface sensitivity on account of the weaker Brewster condition, as shown in figure 2(b).

3.2. Ellipsometry

The complex ellipsometric ratio, ρ , is usually expressed in terms of the ellipsometric angles Ψ and Δ defined by

$$\rho = r_p/r_s = \tan \Psi e^{i\Delta}. \quad (4)$$

Values of Ψ and Δ calculated for a bare Si surface for 45° and 75° incidence are shown by the solid curves in figure 3. Results with a 0.5 nm SiO₂ overlayer are shown as dashed curves. It is clear that enhanced surface sensitivity is obtained for 75° incidence, corresponding to the pseudo-Brewster condition for a photon energy of around 1.5 eV. It is widely appreciated that SE achieves optimum surface sensitivity for incidence around ϕ_B [3].

Corresponding simulations using a Au substrate are shown in figure 4. In this case insignificant enhancement of surface sensitivity is observed for ϕ_B on account of the weaker Brewster minimum in R_p for metals (see figure 2).

For a bare substrate, there is a simple relationship between dielectric function, ϵ , and ellipsometric ratio, allowing, in principle, ϵ to be determined from measurements of ρ . Although ideal semi-infinite substrates do not exist, as discussed at the end of section 2, it is often convenient to interpret ellipsometric data in terms of the ‘two-phase model’ (i.e. vacuum and perfect substrate). The dielectric function deduced in this way is referred to as the ‘effective’ or ‘pseudo-’ dielectric function of the system and is given by

$$\langle \epsilon \rangle = \sin^2 \phi \left(1 + \tan^2 \phi \left[\frac{1 - \rho}{1 + \rho} \right]^2 \right). \quad (5)$$

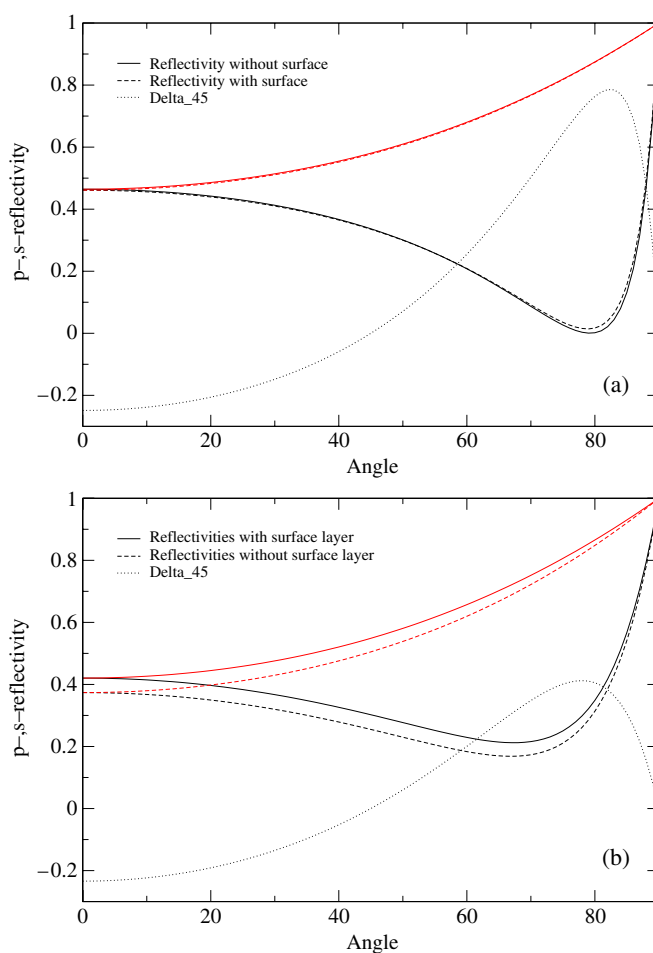


Figure 2. (a) The solid curves show R_s , R_p and Δ_{45} for Si at a photon energy of 3 eV as functions of the angle of incidence ϕ . The dashed curves indicate the corresponding results when a 5 nm thick layer of SiO_2 covers the Si substrate. Also shown (dotted curve) is the variation of $R_s^2 - R_p$ for bare Si with incidence angle. (b) As for (a) except with an Au substrate and Cu overlayer.

$\text{Im}(\epsilon)$ for a 0.5 nm SiO_2/Si system deduced from simulations of ρ at 75° incidence is compared with ϵ_{Si} in figure 5. The effect of the surface film is small but can be seen, and more importantly $\langle \epsilon \rangle$ can be measured reproducibly to three decimal places with current SE instrumentation [4]. Although SE has monolayer sensitivity, unambiguous determination of ϵ_s , the surface dielectric function, is much more difficult. The central problem is that ϕ and ϵ_b , the substrate dielectric function, must be known to high accuracy first, and ϵ_b cannot be measured independently since bare substrates do not exist. It is clear that attempts to deduce surface dielectric response must include a self-consistent determination of ϵ_b . To illustrate the difficulties this presents, the results of two further simulations are shown in the lower graph of figure 3. These are obtained using the measurements of ϵ_{Si} made by Jellison [23] (dot-dashed curve) and Edwards [24] (dotted curve). Corresponding $\text{Im}(\epsilon)$ spectra are included in figure 5. For photon energy greater than 2.5 eV it is immediately apparent that the uncertainty in the assumed values of ϵ_{Si} affect the calculated $\langle \epsilon \rangle$ at least as much as nanometre surface overlayers, even in the case of Si, probably the most intensively studied substrate material.

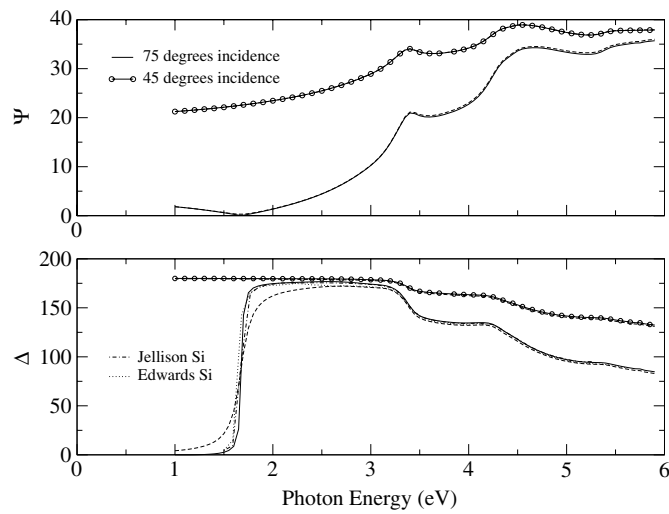


Figure 3. Ellipsometric angles calculated for a bare Si substrate (solid curve) and with a 0.5 nm SiO_2 overlayer (dashed curve). The lower graph includes simulated Δ for substrate data from [23] (dot-dashed curve) and [24] (dotted curve).

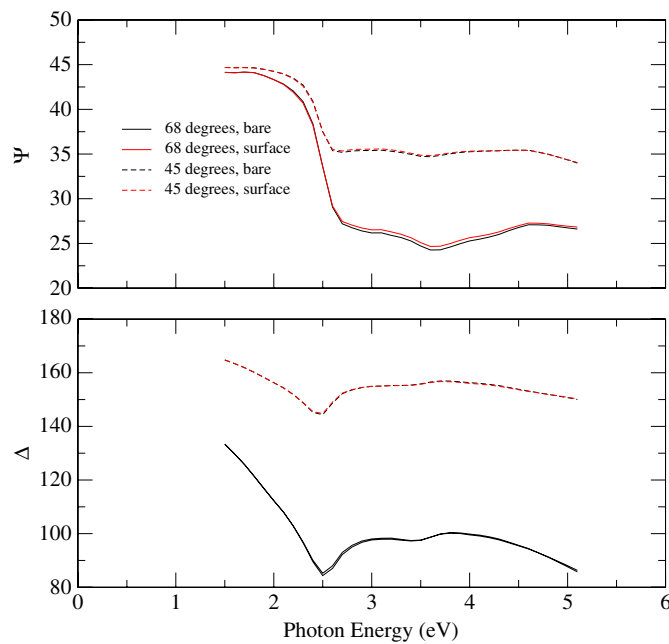


Figure 4. Ellipsometric angles calculated for a 0.5 nm layer of Cu on Au and for a bare Au substrate.

It should be noted that Kelly *et al* [25] have used a novel approach to break the circular problem described above. These authors measured the change in ρ caused by exposure of the atomically clean and reconstructed Si(111) and Si(001) surfaces to atomic hydrogen. On the grounds that H atoms saturate the dangling bonds at the surface, making it approximately

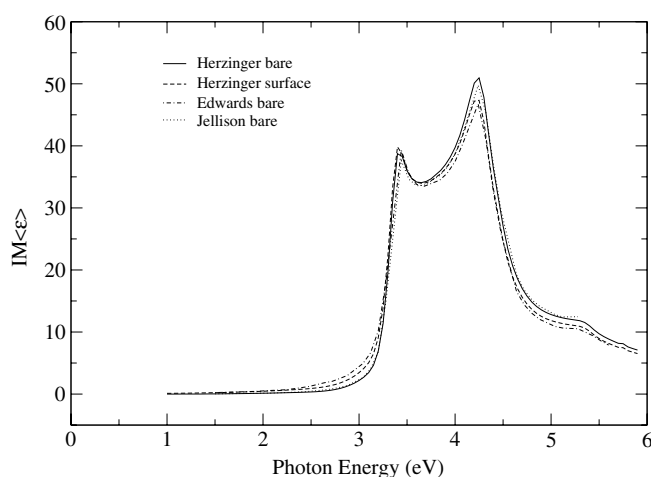


Figure 5. $\text{Im}(\epsilon)$ for 0.5 nm SiO_2 on Si (dashed curve) derived from simulations of ρ utilizing optical constants from [22]. Also shown are estimates of ϵ_{Si} deduced in the ellipsometric studies of Edwards [24] (dot-dashed curve), Jellison [23] (dotted curve) and Herzinger *et al* [22] (solid curve).

bulklike, the change in ρ can be associated with the optical response of the clean reconstructed surfaces.

SE is particularly well suited to tracking the development of epilayers. If material B grows homogeneously on material A then experimental ellipsometric measurements for a series of different overlayer thicknesses can be simulated using a model with a single overlayer and the material dielectric functions determined by numerical fitting. The failure of such an approach motivates a more sophisticated treatment and in this way Herzinger *et al* [22] have found indirect evidence for the presence of a thin (~ 1 nm) interface region between bulk Si and stoichiometric oxide overlayers. Even in this detailed multi-sample study the nature of the interface layer could not be identified and alternative interpretations of the experimental data cannot be ruled out, e.g. non-locality of the dielectric function at the interfaces [27], neglected by construction in the stratified medium approach. Thus we summarize this section by noting that SE has undoubted submonolayer surface sensitivity, but the determination of surface and interface optical response remains a challenge.

3.3. 45 degree reflectometry

For any bare isotropic substrate Δ_{45} is identically zero. The Δ_{45} spectra for a series of SiO_2 thin films on Si are shown in figure 6. The solid, dotted and dashed curves were calculated using ϵ_{Si} from [22, 23] and [24], respectively. The observed insensitivity to uncertainties in the substrate dielectric function implies 45DR is well suited to fundamental studies of surface optical response at the sub-monolayer level. To illustrate this we have fitted the Δ_{45} spectrum simulated using a 0.5 nm SiO_2 overlayer and ϵ_{Si} from [22] using the ϵ_{Si} of [23] and [24] as input and the dielectric function of the overlayer as a free parameter. The correct and fitted values of the real part of ϵ_{SiO_2} are plotted in figure 7. (SiO_2 is non-absorbing in our spectral range.) Without any special methodology the surface dielectric function is reproduced reasonably well. Equivalent treatment of ellipsometric data yields relatively poor results, as shown by the relevant curves (triangles and circles) in figure 7. Indeed, to deal numerically with erroneous bulk data it is necessary to introduce non-physical negative ϵ_{SiO_2} .

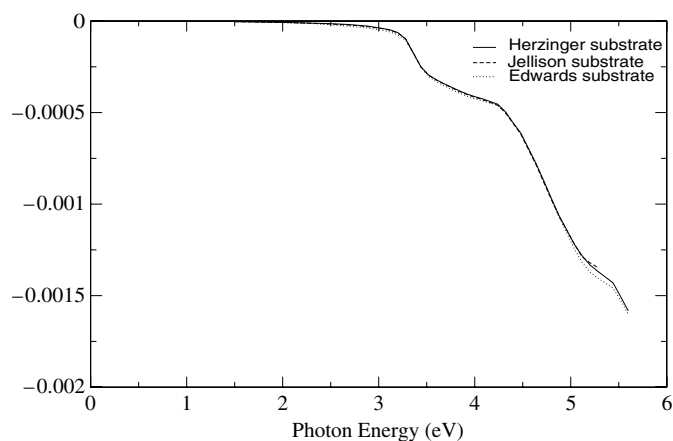


Figure 6. Simulated Δ_{45} spectra for 0.5 nm SiO_2 on Si. ϵ_{Si} has been taken from [22] (solid curve), [23] (dashed curve) and [24] (dotted curve).

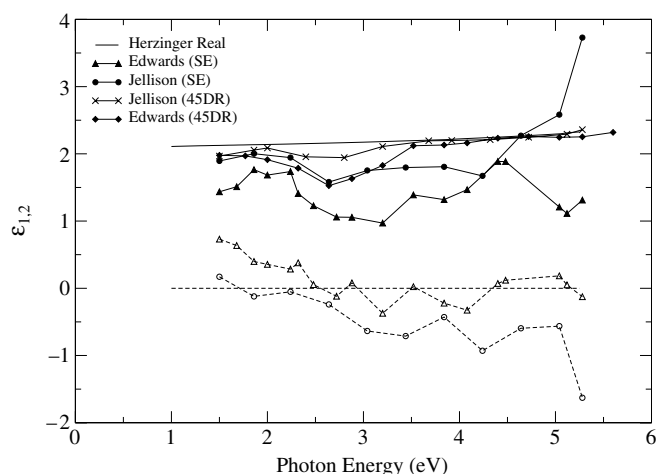


Figure 7. The solid (dashed) curves show the real (imaginary) part of ϵ_{SiO_2} calculated via simulations using data taken from [22] which are then inverted for ϵ_{SiO_2} using data from [23] and [24] by fitting for either ellipsometric or 45DR data.

As an aside, we note that numerical fitting can in theory be avoided by appeal to the ‘thin film limit’ [26] in which Δ_{45} is expanded to first order in d/λ :

$$\Delta_{45} \approx -4\pi\sqrt{2}R_p^{(d=0)}\frac{d}{\lambda}\text{Im}\left\{\frac{(\epsilon_s - \epsilon_b)^2}{\epsilon_s(\epsilon_b - 1)^2}\right\}. \quad (6)$$

Simulations of Δ_{45} for a 0.5 nm SiO_2 overlayer on Si using the thin film approximation in equation (6) have an accuracy of $\sim 3\%$. However, extraction of ϵ_s by inverting equation (6) gives poor results, even if the correct ϵ_b is used, unless an unphysically thin surface region is assumed.

The dotted curves in figure 2 show the variation in $R_s^2 - R_p$ with angle of incidence ϕ . The slope of the curve around $\phi = 45^\circ$ suggests that 45DR is rather unforgiving of errors in ϕ . In fact, this problem is common to other reflection spectroscopies including SE. Rossow

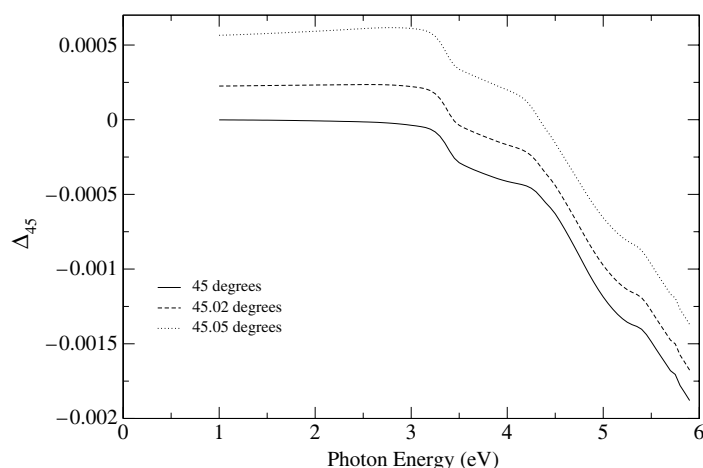


Figure 8. Δ_{45} spectra for 0.5 nm SiO_2 on Si for $\phi = 45.00^\circ, 45.02^\circ, 45.05^\circ$.

and Richter have pointed out [4] that inversion of equation (5) using a value of ϕ in error by 0.05° , the typical experimental uncertainty for SE, leads to an error in $\langle\epsilon\rangle$ of order 0.1. Such systematic errors ensure that the accuracy of ellipsometric measurements does not approach their precision. Concerning experimental RAS measurements, $\phi \approx 3^\circ$ as opposed to true normal incidence is usual. Berreman simulations for bare isotropic substrates such as Si and Au yield $\Delta r/r$ spectra with magnitude 10^{-3} for $\phi = 3^\circ$ with the plane of incidence along x . While this ellipsometric effect is comparable in magnitude to the typical RAS signals derived from anisotropic surfaces, it can be essentially eliminated by choosing the x and y directions so that the plane of incidence bisects them. In 45DR an error of $\Delta\phi \sim 0.05^\circ$ leads to an error in Δ_{45} which is smaller than but comparable to the magnitude of Δ_{45} itself. Simulated results for 0.5 nm of SiO_2 on Si shown in figure 8 suggest that incidence errors become tolerable for $\Delta\phi \approx 0.02^\circ$. Thus the instrumental requirements of implementing 45DR are rather strong.

4. Conclusion

Since both ρ and Δ_{45} can vanish for bare substrates, one might suppose that 45DR offers similar information to SE. Certainly both SE and 45DR require ϕ to be set with high accuracy if measurements are to correctly interpreted. It is clear that for metals, and above the optical gaps of semiconductors, ρ does not vanish and 45DR has distinctly greater surface sensitivity. Even for non-absorbing materials 45DR has the advantage that the required experimental geometry, i.e. $\phi = 45^\circ$, is independent of material properties and photon energy, while ϕ_B is not. In fact SE is usually operated a few degrees away from ϕ_B so as to avoid the $\rho \rightarrow 0$ condition [3]. While surface specific techniques dominate their niche, SE remains the premier optical characterization tool for thin films. 45DR lies in the former category but modern variable-angle ellipsometers could be used to measure Δ_{45} . Indeed it may be the case that Δ_{45} measurements could be used as additional constraints in the numerical fitting of SE data. Thus 45DR and SE are complementary.

Linear optical techniques for surface studies combine versatility with simplicity and economy and are therefore well suited to the role of real time diagnostic. Since rather few analytical techniques can serve this purpose, surface sensitive reflection spectroscopies continue to make a substantial impact in surface science. The last decade has seen a major

advance in the theoretical description of surface optical response [27] and this has been motivated primarily by the wealth of experimental results obtained with the surface specific optical techniques SDR and RAS. 45DR offers the surface specificity of RAS and SDR without the need for reference surfaces or anisotropic surface layers. Development of 45DR should increase the flexibility of reflection techniques for *in situ* surface monitoring, and offer something new to both the surface-specific and thin film communities.

Acknowledgments

This work was supported by The Royal Society and the EPSRC.

References

- [1] Cardona M 1969 *Modulation Spectroscopy (Solid State Physics suppl. 11)* (New York: Academic)
- [2] See for example, Ruzgas T, Wong L, Gaigalas A K and Vilker V L 1998 *Langmuir* **14** 7298
- [3] Azzam R M A and Bashara N M 1977 *Ellipsometry and Polarized Light* (Amsterdam: North-Holland)
- [4] Rossow U and Richter W 1995 *Optical Characterization of Epitaxial Semiconductor Layers* ed G Bauer and W Richter (Berlin: Springer)
- [5] McGilp J F 1995 *Prog. Surf. Sci.* **49** 1
- [6] Chiaradia P, Chiarotti G, Ciccacci F, Memeo R, Nannarone S, Sassaroli P and Selci S 1980 *Surf. Sci.* **99** 7011
- [7] Chiaradia P, Cricenti A, Selci S and Chiarotti G 1984 *Phys. Rev. Lett.* **52** 1145
- [8] Selci S, Chiaradia P, Ciccacci F, Cricenti A, Sparvieri N and Chiarotti G 1985 *Phys. Rev. B* **31** 4096
- [9] Bleckman L, Hunderi O, Richter W and Wold E 1996 *Surf. Sci.* **351** 277
- [10] Aspnes D E 1997 *Solid State Commun.* **101** 85
- [11] Maytorena J A, Lopez-Bastidas C and Mochan W L 1998 *Phys. Status Solidi b* **170** 337
- [12] Madrigal-Melchor J, Perez-Rodriguez F, Maytorena J A and Mochan W L 1997 *Appl. Phys. Lett.* **71** 69
- [13] Silvio-Castillo A and Perez-Rodriguez F 1999 *J. Appl. Phys.* **86** 1404
- [14] Silvio-Castillo A and Perez-Rodriguez F 2000 *Phys. Status Solidi b* **219** 215
- [15] Silvio-Castillo A and Perez-Rodriguez F 2001 *J. Appl. Phys.* **90** 3662
- [16] Teitler S and Henvis B 1970 *J. Opt. Soc. Am.* **60** 830
- [17] Berreman D W and Scheffer T J 1970 *Phys. Rev. Lett.* **25** 577
- [18] Berreman D W 1972 *J. Opt. Soc. Am.* **62** 502
- [19] Schubert M 1996 *Phys. Rev. B* **53** 4265
- [20] See for example, Shurcliff W A and Ballard S S 1964 *Polarized Light* (Princeton, NJ: Van Nostrand-Reinhold)
- [21] Kobayashi N and Horikoshi Y 1989 *Japan. J. Appl. Phys.* **28** L1880
- [22] Herzinger C M, Johs B, McGahan W A, Woollam J A and Paulson W 1998 *J. Appl. Phys.* **83** 3323
- [23] Jellison G E Jr 1992 *Opt. Mater.* **1** 41
- [24] Edwards D E 1985 *Handbook of the Optical Constants of Solids* ed E D Palik (Orlando, FL: Academic)
- [25] Kelly M K, Zollner S and Cardona M 1993 *Surf. Sci.* **285** 282
- [26] McIntyre J D E and Aspnes D E 1971 *Surf. Sci.* **24** 417
- [27] del Sole R 1998 *Thin Solid Films* **313** 527